One-step 3D microstructuring of PMMA using MeV light ions

Oleksandr Romanenko[1*], *Adela* Jagerova[1,2], *Andrei* Borodkin[3], *Vladimir* Havranek[1] and *Anna* Mackova[1,2]

[1]Nuclear Physics Institute, Czech Academy of Sciences, 25068 Rez, Czech Republic
[2]J. E. Purkinje University, 40096 Usti nad Labem, Czech Republic
[3]Institute of Photonics and Electronics, Czech Academy of Sciences, 18251 Prague, Czech Republic

Abstract. The conventional procedure for creating 3D microstructures in resists by ion beam lithography consists of two stages – exposure and developing. However, single stage of manufacturing 3D structures in resist is also possible. Irradiation of PMMA can cause it to shrink. This feature of the polymer can be used for one-step three-dimensional microstructuring, which simplifies the manufacturing process. The shrinkage of PMMA film on a substrate has been extensively studied, while research on free-standing film is not comprehensive. The use of free-standing PMMA film allows the creation of a flexible material with 3D microstructures, which can be used in medicine, optics, and electronics. The question here is whether the results obtained for the PMMA film on the substrate are applicable to the free-standing film. Since the nature of shrinking is outgassing of volatile products, the film on the substrate has only one surface for the release of gases, while in the free-standing film, gases can be released from the sample from both sides. Therefore, the shrinking in the free-standing film occurs on both sides. The aim of this work is to study the shrinkage of the free-standing film and compare it with that of the film of the same thickness coated on the substrate.

Conventional ion beam lithography as well as direct (maskless) ion beam lithography follow two steps: 1) irradiation of material; 2) developing the material with chemical reagents. As result, 3D structures in the material can be created. PMMA, PDMS and SU-8 are the most used the polymers in ion beam lithography. It has been shown that microlenses can be formed in PDMS with direct ion beam lithography using heavy ions such as Nitrogen without chemical development [1]. This is possible to do due to the property of PDMS to shrink under irradiation. PMMA also shrinks when exposed to an ion beam [2,3]. Such behaviour of the polymers is explained by the leaving of volatile products from the material [4]. H_2, CO, CO_2 and CH_4 are the main gases produced in PMMA during irradiation, which subsequently diffuse from the material [5-7]. This feature can be exploited to simplify the production of the optical devices made of the polymer.

The flexibility of the optical devices is gaining in importance. This for example allows creating the digital cameras that mimic compound eyes commonly found in insects or spiders

* Corresponding author: romanenko@ujf.cas.cz

and are characterized by extremely large field of view angle, low aberrations, acute sensitivity to motion, and infinite depth of field [8]. In case of the polymer, a flexible sample can be obtained in two ways: i) using a flexible substrate; ii) making the sample thin enough to be flexible, which means producing a free-standing polymer film. If two polymer films of the same thickness are prepared by these two methods and exposed to ion beam irradiation, they will most likely have different shrinkage. This can be explained as follows: as already mentioned, the cause of shrinkage is the degassing of volatile products. These products can diffuse out of the sample from only one side in the case of the film on the substrate, while in the case of the free-standing film, they can diffuse from both sides of the sample, causing the polymer to shrink on both sides. This is schematically illustrated in Fig 1.

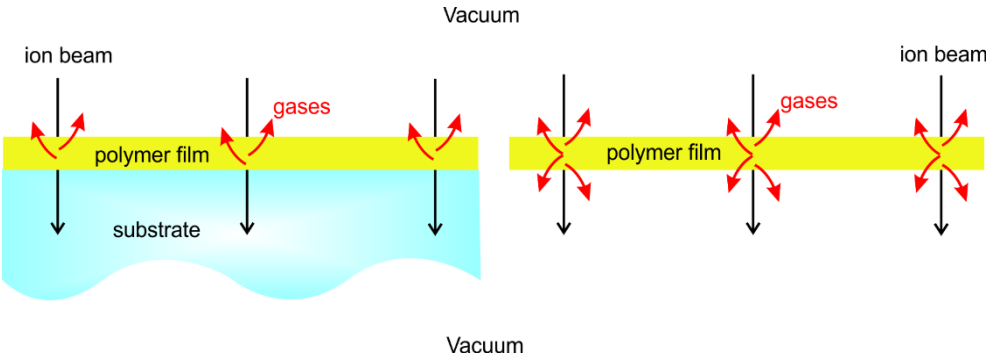

Fig. 1. Schematic illustration of the degassing of the polymer film.

In our work, we demonstrate the applicability of one-step three-dimensional microstructuring for the fabrication of the optical device created by irradiation alone. We also demonstrate the difference in structures created in the film on the substrate and the free-standing film irradiated under the same conditions. For our goals, we used PMMA because of its good optical transparency in visible light, easy handling and low cost.

Our samples were prepared as follows: 1 g of PMMA powder and 7.67 g of acetone were mixed in a vial with a magnetic stirrer. When PMMA was completely dissolved in acetone, the solution was spin-coated on the polyethylene and glass substrates using 400 rpm for 100 s. The PMMA film on polyethylene was subsequently peeled off to obtain the free-standing flexible PMMA film. The thickness of both the PMMA film on glass and the free-standing PMMA film was 20 μm. Irradiation was carried out on a nuclear microbeam facility at our institute[9]. 2 MeV proton beam focused into a spot of 0.77×2.37 μm^2 with a beam current of 68 pA were used to irradiate the samples. Diffraction grating of 100 lines/mm was chosen as the optical device to demonstrate the applicability of the method. The irradiation parameters were set as follows: the dose – 400 nC/mm^2 (2.5E14 protons/cm^2), scan size – 1024×1024 pixels, pixel dimension – 1×1 μm^2. To reduce the heating effect caused by irradiation, the irradiated pattern was created by scanning in 11 loops. This increases the time required for irradiation, but reduces the heat load well. The total time spent on one diffraction grating was 632 s.

The thickness of the film and the energy of the protons were chosen in such a way that the protons transfer their energy to PMMA uniformly over the entire depth of the film. SRIM program [10] for modelling the interaction of ions with the material shows that the difference of linear energy transfer (LET) of 2 MeV protons in PMMA is about 15 % between the front and the back side of the film (Fig. 2).

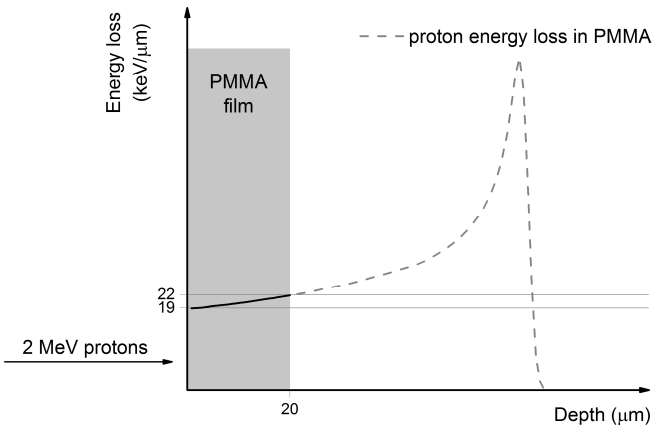

Fig. 2. Linear Energy Transfer of 2 MeV protons in PMMA. The solid line shows the protons energy losses in the prepared PMMA film.

Optical analysis of the irradiated samples revealed distinct lines corresponding to the places of interaction of the proton beam with the material (Fig. 3). The quality of the created gratings were good, although some inclusions were noticed. We assume that the appearance of inclusions was caused by fluctuation in the proton beam current. Despite the 11-loops scan, which smooths out fluctuations in the beam current and thus makes the irradiation load more uniform, some pixels received noticeably higher fluence than others. This can be explained in the following way: The time spent in every pixel was the same, therefore those pixels that were exposed to the beam when it had the high current accumulated the higher fluence compared to others. If this happened in every loop, the final fluence in such pixels was greater than in others. This problem can be eliminated by increasing the number of scan loops, but this will increase the irradiation time [2]. Visually, the width of the lines appears to be greater than the beam width of 0.77 μm, although precise lines width measurements were not possible on the obtained optical images. For this it was better to use AFM.

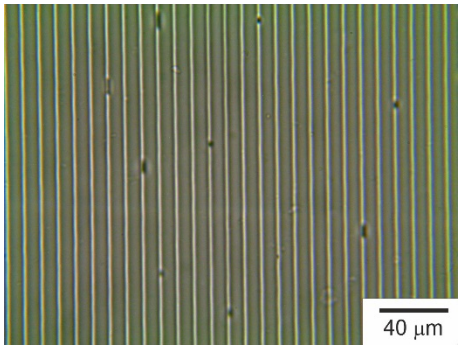

Fig. 3. Optical image of irradiated PMMA film on glass.

AFM analysis was used to investigate the topography of the irradiated area. As can be seen in Fig. 4, shrinkage in the film coated on glass was more pronounced than in the free-standing film. The profile of the grating created in the film on glass shows that the depth of the grooves was 160 nm (Fig. 5). In case of the free-standing film, the depths of the grooves were 9 and 11 nm on the front and back sides of the film, respectively. The difference in grooves depth between front and back sides is explained by LET, that increases with depth. The total shrinkage of PMMA in the free-standing film is 20 nm, which is almost an order of

magnitude lower than that for PMMA film on glass. The reason of such big difference is unclear.

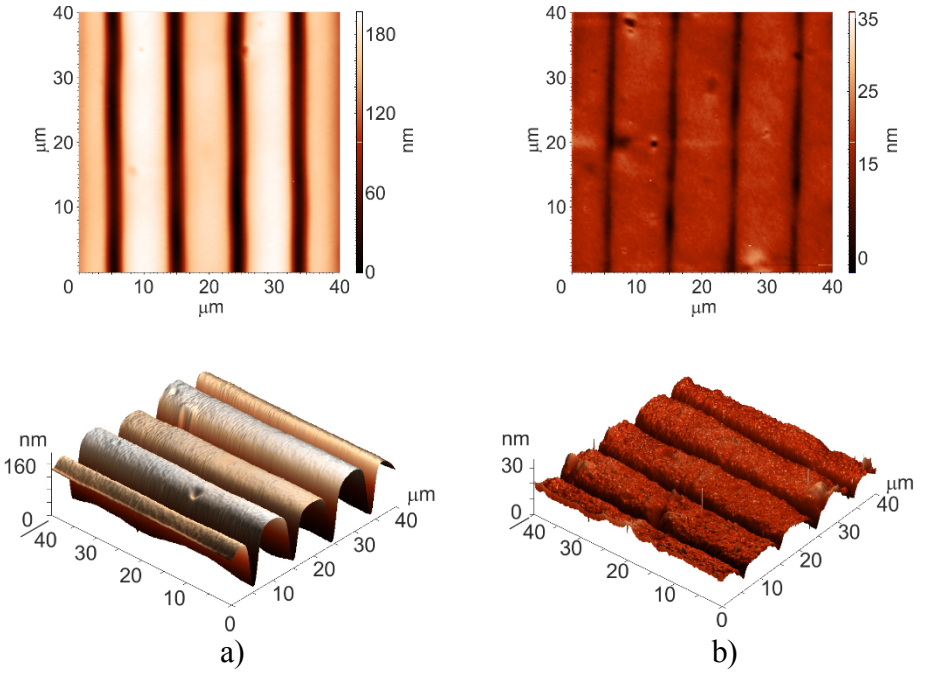

Fig. 4. AFM images of the PMMA films irradiated with the same condition: a) PMMA film on glass; b) free-standing PMMA film (front side).

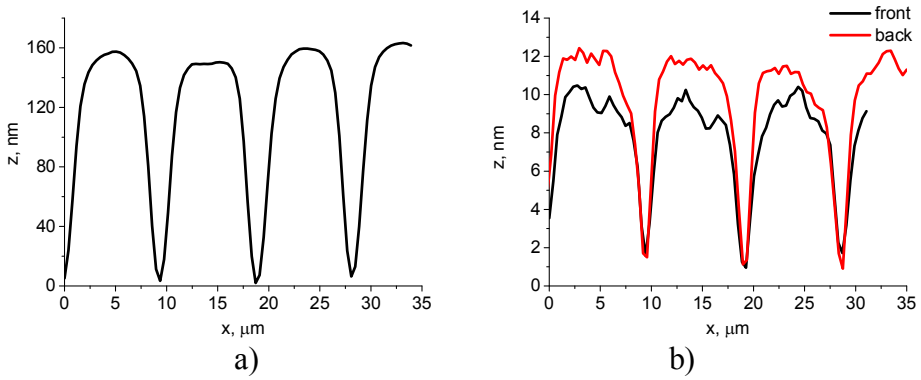

Fig. 5. Profiles of the created diffraction gratings showing PMMA shrinkage: a) PMMA film on glass; b) free-standing PMMA film.

From Fig. 4 it seems that the roughness of unirradiated area in the free-standing film is higher than that in the film on glass, but this is just illusion caused by the difference in scale. Analysis of unirradiated area revealed that its roughness is about 1.6 nm for both samples.

Gaussian fit, implemented in the OriginPro software, was used to analyze the profile of the grooves in PMMA. It was found that FWHM of the grooves in PMMA on glass is 2.23 μm, and in free-standing PMMA – 1.76 μm. This difference is explained by the different depth of the grooves. When the polymer shrinks in the place exposed to the ion beam, it pulls

along the unirradiated part of the material adjacent to it. Thus, the more the polymer shrinks, the more it pulls the undamaged material with it, which leads to a widening of the groove.

To check the quality of the created diffraction grating, monochromatic light with vertical polarization and a wavelength of 520 nm was utilized. An interference pattern was obtained on a screen located at a distance of 50 cm from the diffraction grating (Fig. 6). Close look on the interference pattern shows parasitic flare. This was observed for both samples, although in the case of the PMMA film on glass, parasitic flare was less noticeable. Such parasitic flare is caused by defects in the diffraction grating. The quality of the diffraction grating can be assessed by the intensity of the fringes. Table 1 shows the measured fringe intensities. As can be seen, the ratio between the zeroth and other orders is greater in the PMMA film on glass, which means a better quality of diffraction grating compared to a free-standing PMMA film.

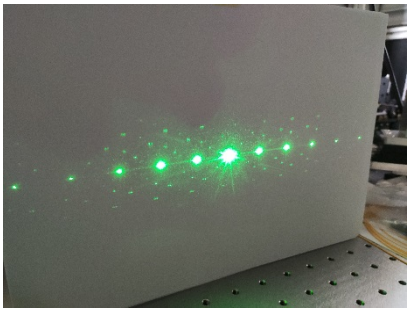

Fig. 6. Interference pattern obtained with created diffraction grating in the free-standing PMMA film.

Table 1. Intensity of fringes in the interference patterns obtained with the created diffraction gratings.

Fringe order	**Intensity, μW Free-standing PMMA film**	**Intensity, μW PMMA film on glass**
0	600	860
+1	112	22
-1	114	27
+2	55	27
-2	59	30
+3	12	12
-3	14	12

Interference pattern allows the period of diffraction grating be evaluated. Calculated period for every order is presented in Table 2. The fluctuation of the values is less than 5% and is associated with an error in the selection of the center of the fringe during the measurement. The pattern for irradiation was 100 lines/mm which gives the period of the diffraction grating of 10 μm. Thus, the created diffraction grating reproduces the original pattern with high accuracy.

To summarize, it was shown that one-step 3D microstructuring of the polymer using MeV light ions is viable. 3D microstructures in PMMA have been successfully created with 2 MeV protons in a single step. The application of this approach has been demonstrated by the example of the production of the optical device – the diffraction grating. The fabricated diffraction grating showed good agreement with the original pattern. The structures quality was good, with some minor artifacts, which can be eliminated by changing the scanning

method. One-step microstructuring simplifies the manufacturing procedure and has great potential for prototyping new optical devices.

Table 2. The period of the diffraction gratings calculated from the interference pattern.

Fringe order	Free-standing PMMA film		PMMA film on glass	
	Distance from zeroth order, mm	Calculated grating period, µm	Distance from zeroth order, mm	Calculated grating period, µm
+1	26	10.01	25	10.41
-1	26	10.01	26	10.01
+2	53	9.88	52	10.07
-2	53	9.88	53	9.88
+3	81	9.79	79	10.03
-3	79	10.03	81	9.79

The research has been carried out at the CANAM (Centre of Accelerators and Nuclear Analytical Methods) infrastructure LM 2015056. This publication was supported by OP RDE, MEYS, Czech Republic under the project CANAM OP, CZ.02.1.01/0.0/0.0/16_013/0001812 and by the Czech Science Foundation (GACR No. 19-02482S)

References

1. G. U. L. Nagy, V. Lavrentiev, I. Banyasz, S. Z. Szilasi, V. Havranek, V. Vosecek, R. Huszank, I. Rajta, Thin Solid Films **636**, 634 (2017).
2. O. Romanenko, V. Havranek, P. Malinsky, P. Slepicka, J. Stammers, V. Svorcik, A. Mackova, D. Fajstavr, Nucl. Instrum. Methods B **461** 175 (2019)
3. T. C. Sum, A. A. Bettiol, H. L. Seng, I. Rajta, J. A.van Kan, F. Watt, Nucl. Instrum. Methods B **210** 266 (2003)
4. F. Schrempel, Y.-S. Kim, W. Witthuhn, Appl. Surf. Sci. **189** 102 (2002)
5. B. Pignataro, M.E. FragalB, O. Puglisi, Nucl. Instrum. Methods B **131** 141 (1997)
6. E. H. Lee, G. R. Rao, L. K. Mansur, Radiat Phys Chem **55** 293 (1999)
7. Z. Chang, J. A. LaVerne, Radiat. Phys. Chem. **62** 19 (2001)
8. Y. M. Song, Y. Xie, V. Malyarchuk, J. Xiao, I. Jung, K. Choi, Z. Liu, H. Park, C. Lu, R. Kim, R. Li, K. B. Crozier, Y. Huang, J. A. Rogers, Nature **497,** 95–99 (2013)
9. O. Romanenko, V. Havranek, A. Mackova, M. Davidkova, M. Cutroneo, A. G. Ponomarev, G. Nagy, J. Stammers, Rev. Scient. Instr. **90** 013701 (2019)
10. J. F. Ziegler, M. D. Ziegler, J. P. Biersack, Nucl. Instrum. Methods B **268** 1818 (2010)